International Journal of Nanomedicine

Dovepress
open access to scientific and medical research

Open Access Full Text Article

ORIGINAL RESEARCH

Biosynthesis, characterization, and evaluation of bioactivities of leaf extract-mediated biocompatible silver nanoparticles from an early tracheophyte, *Pteris tripartita* Sw.

This article was published in the following Dove Press journal:
International Journal of Nanomedicine
14 November 2016
Number of times this article has been viewed

Xavierravi Baskaran[1]
Antony Varuvel Geo Vigila[2]
Thangaraj Parimelazhagan[3]
Doulathabad Muralidhara-Rao[4]
Shouzhou Zhang[1]

[1]Shenzhen Key Laboratory of Southern Subtropical Plant Diversity, Fairy Lake Botanical Garden, Shenzhen and Chinese Academy of Sciences, Shenzhen, People's Republic of China; [2]Department of Zoology, St Xavier's College, Palayamkottai, [3]Department of Botany, Bioprospecting Laboratory, Bharathiar University, Coimbatore, Tamil Nadu, [4]Department of Biotechnology, Sri Krishnadevaraya University, Anantapur, Andhra Pradesh, India

Abstract: The objective of the study was to characterize silver nanoparticles (Ag-NPs) and their bioactivities in early tracheophytes (Pteridophyta). Aqueous leaf extract of a critically endangered fern, *Pteris tripartita* Sw., was used for one-step green synthesis of Ag-NPs. The biosynthesized Ag-NPs were characterized using ultraviolet-visible spectroscopy, Fourier transform infrared spectroscopy, scanning electron microscopy, energy-dispersive X-ray spectroscopy, X-ray diffraction, and high-resolution transmission electron microscopy. Morphologically, the Ag-NPs showed hexagonal, spherical, and rod-shaped structures. Size distributions of Ag-NPs, calculated using Scherrer's formula, showed an average size of 32 nm. Ag-NPs were studied for in vitro antioxidant, antimicrobial, and in vivo anti-inflammatory activities. Ag-NPs exhibited significant anti-inflammatory activity in carrageenan-induced paw volume tests performed in female Wistar albino rats. Furthermore, Ag-NPs showed significant antimicrobial activity against 12 different microorganisms in three different assays (disk diffusion, time course growth, and minimum inhibitory concentration). This study reports that colloidal Ag-NPs can be synthesized by simple, nonhazardous methods, and that biosynthesized Ag-NPs have significant therapeutic properties.

Keywords: silver nanoparticles, *Pteris tripartita*, FTIR, HRTEM, antioxidant, antimicrobial

Introduction

Generally, nanoparticles (NPs) are colloidal systems with particles varying in size from 10 to 1,000 nm.[1] At present, there are plenty of nanotechnology products commercially available.[2,3] While physical, chemical, and biological methods are all available for the synthesis of NPs, at present, chemical approaches are most commonly used. However, these chemical synthesis methods are expensive and require the use of toxic chemicals. Thus, synthesis of NPs from biomolecules of microbes and plants has become a more common method in recent years. Previous studies have identified biomolecules including proteins, polyphenols, flavonoids, and other phytochemicals that have an ability to reduce ions to nanosize and to stabilize NPs by acting as capping agents.[4] Noble metal NPs with gold, silver, and platinum have been widely used for many years; hence, there is an urgent need to develop an ecofriendly method of synthesizing noble metal NPs without using toxic chemicals.

In particular, silver compounds are widely used for healing purposes owing to their antimicrobial properties.[5,6] Historically, Alexander the Great also used silver vessels

Correspondence: Shouzhou Zhang
Shenzhen Key Laboratory of Southern Subtropical Plant Diversity, Fairy Lake Botanical Garden, Shenzhen and Chinese Academy of Sciences, 165 Xianhu Road, Shenzhen 518004, People's Republic of China
Tel +86 755 180 2539 1959
Email shouzhouz@126.com

submit your manuscript | www.dovepress.com
Dovepress
http://dx.doi.org/10.2147/IJN.S108208

to store drinking water.[7] In earlier studies, microorganisms,[8] enzymes,[9] fungi,[10] and some plant extracts[11–14] have also been widely used in NP biosynthesis; their use suggests the possibility of developing an ecofriendly NP synthesis method to replace chemical and physical methods. Gardea-Torresdey et al[15] reported the formation of gold and silver NPs (Ag-NPs) by living plants for the first time. NP synthesis using plants has distinct advantages over microbial synthesis: this method is rapid, of single step, low cost, and has notable ecofriendly properties. Moreover, plant NP synthesis also eliminates the expensive and time-consuming process of maintaining cell cultures for large-scale NP synthesis.[16] In our earlier studies, we assessed spore germination percentage, gametophyte growth, apogamous sporophyte development, phytochemical, in vitro antioxidant, and in vivo anti-inflammatory activity of *Pteris tripartita* Sw. extracts.[17–21] Even though this plant has been widely discussed for its potential medicinal uses, to date, the biosynthesis of Ag-NPs using pteridophyte (fern) extracts has not been reported. Thus, the main objective of our present study was to biosynthesize Ag-NPs using an aqueous leaf extract of *P. tripartita* Sw., and to assess these extracts for antioxidant, anti-inflammatory, and antimicrobial properties through in vitro and in vivo assays.

Materials and methods

Collection of plant material

Mature leaves of *P. tripartita* Sw. without spores were collected from the Nuburagangai stream of Alagar Hills (altitude: 500–750 m) in Madurai District, Tamil Nadu, India. Voucher specimens were numbered, authenticated (XCH 25403), and deposited in St Xavier's College Herbarium, Palayamkottai (Tamil Nadu, India). The plant material was washed in running tap water in order to remove the dust and shade-dried at room temperature. The dried plant material was coarsely powdered and stored in a plastic container for further processing.

Plant extraction

Leaf broth solution was prepared by combining 5 g of plant powder with 100 mL of double-distilled water in a 250 mL Erlenmeyer flask and boiling the mixture for 5 minutes, followed by filtering the reaction mixture through Whatman No 1 filter paper. The filtrate was stored at 4°C and used within a week (in order to reduce contamination of the plant aqueous extract).[22]

Biosynthesis of Ag-NPs

Ultraviolet-visible spectroscopy and Fourier transform infrared spectroscopy analysis

Silver nitrate ($AgNO_3$) was purchased from Sigma-Aldrich Co. (St Louis, MO, USA) and a 1 M solution of $AgNO_3$ was prepared. Two milliliters of the plant extract was mixed with 1,000 mL of 1 M $AgNO_3$ solution and the mixture was kept at room temperature for 24 hours to obtain a reddish-brown suspension. Observations were made through ultraviolet-visible (UV–vis) spectroscopy (Model: Lambda 35; PerkinElmer Inc., Waltham, MA, USA). The suspension was also analyzed using a Fourier transform infrared (FTIR) spectrophotometer (Model Spectrum RX1, PerkinElmer Inc.) at a range of 4,000 to 400 cm^{-1}. To collect NPs, the reaction mixture was centrifuged (Eppendorf 5804R (Eppendorf 5804R, Germany) twice at 10,000 rpm for 10 minutes each. The supernatant was then discarded. In order to acquire pure NPs, free of unwanted biological materials, the pellet was washed with 1 mL of double-distilled water, centrifuged twice, and dried on a watch glass at room temperature. Finally, the Ag-NPs were then stored at 4°C for further studies.[23]

Characterization of Ag-NPs using scanning electron microscopy and energy-dispersive X-ray analysis

Scanning electron microscopy (SEM) and energy-dispersive X-ray analysis (EDAX) were performed using a JEOL JSM-6390 model at 20 kV. Thin films of the sample were prepared on a carbon-coated copper grid by dropping a very small amount of the sample on the grid, and extra moisture was removed using blotting paper. Finally, the sample film on the SEM grid was allowed to dry under a mercury lamp for 5 minutes prior to analysis.[23]

High-resolution TEM analysis

High-resolution transmission electron microscopy (HRTEM) is a microscopy technique in which a beam of electrons gets transmitted through an ultrathin specimen and interacts with the specimen. The sample was dispersed in double-distilled water and a drop of thin dispersion was placed on a "staining mat". The carbon-coated copper grid was inserted such that the coated side was turned upward. Ten minutes later, the grid was removed and air dried to screen the NPs using HRTEM (FEI Tecnai G2 F30 S-Twin, Hillsborough, OR, USA) at an accelerating voltage of 80 kV. The magnified image was formed by using an imaging device to capture the interaction of electrons transmitted through the specimen.[23]

X-ray diffraction analysis

The Ag-NPs were drop-coated onto glass substrates to measure their sizes with X-ray diffraction (XRD) using a Shimadzu XRD-6000 instrument. After evaporation of water at room temperature, the dried mixture was assayed to confirm the presence of Ag-NPs. The X-ray diffractometer

operated at 40 kV voltage and 30 mA current with Cu Kα radiation in a θ–2θ configuration.

In vitro antioxidant activities

DPPH radical scavenging activity

Radical scavenging activity of biosynthesized Ag-NPs was measured by the DPPH radical scavenging method described by Blois.[24] Ag-NPs at various concentrations were transferred to test tubes and their volume was adjusted to 100 µL with double-distilled water. Then, 5 mL of 0.1 mmol/L ethanolic solution of DPPH was added and each tube was shaken vigorously. The tubes were allowed to stand for 20 minutes in dark at room temperature. A negative control was prepared as above without Ag-NPs. The absorbance of the samples was measured at 517 nm using a spectrophotometer (Hitachi U-2000). The antioxidant capacities of the samples exposed to DPPH in this assay were compared with those of butylated hydroxyanisole, butylated hydroxytoluene, rutin, quercetin, and a blank. Radical scavenging activity was expressed as the inhibition percentage of free radicals by the samples relative to the control, and was calculated using the following formula: percentage of radical scavenging activity = (control optical density [OD] − sample OD/control OD) ×100.

Chelating activity

The chelation activity of ferrous ions by biosynthesized Ag-NPs was estimated by the method of Dinis et al.[25] First, Ag-NP samples (20 µL) were added to a solution of 2 mmol/L $FeCl_2$ (0.05 mL). The reaction was initiated by the addition of 5 mmol/L ferrozine (0.2 mL) solution. The mixture was shaken vigorously and left to stand at room temperature for 10 minutes. The absorbance of the solution was thereafter measured spectrophotometrically at 562 nm. The chelating activity of Ag-NPs was evaluated using ethylene diaminetetraacetic acid (EDTA) as a standard. The results were expressed as mg EDTA equivalent/g extract. The percentage of inhibition of ferrozine–Fe^{2+} complex formation was calculated using the following equation: $[(A_0 - A_1)/A_0] \times 100$, where A_0 is the absorbance of the control and A_1 is the absorbance of the extract/standard.

Phosphomolybdenum assay

The antioxidant activity of Ag-NPs was evaluated by the phosphomolybdenum method as per Prieto et al.[26] An aliquot of 50 µL of the sample solution (1 mM in dimethyl sulfoxide) was added to a 4 mL vial and combined with 1 mL of reagent solution (0.6 M sulfuric acid, 28 mM sodium phosphate, and 4 mM ammonium molybdate). The vials were capped and incubated in a water bath at 95°C for 90 minutes. After cooling to room temperature, the absorbance of the mixture was measured at 765 nm against a blank. The results were reported in ascorbic acid equivalents (AAE) per gram sample.

Azinobis 3-ethylbenzothiazoline-6-sulfonate ($ABTS^{\cdot+}$) assay

An ABTS radical cation decolorization assay of Ag-NPs, performed according to the method of Re et al,[27] was used to estimate the total antioxidant activity of the samples. $ABTS^{\cdot+}$ was produced by reacting 7 mM $ABTS^{\cdot+}$ aqueous solution with 2.4 mM potassium persulfate in the dark for 12–16 hours at room temperature. The reagent solution was diluted in ethanol (about 1:89 v/v) and equilibrated at 30°C to give an absorbance of 0.7±0.02 at 734 nm. One milliliter of diluted $ABTS^{\cdot+}$ solution was added to different concentrations of the sample or Trolox standards (final concentration 0–15 µM) in ethanol, and absorbance was measured at 30°C exactly 30 minutes after the initial mixing. Three technical replicates were used for each sample dilution. Absorbances were measured at 734 nm and these readings were plotted as a function of Trolox concentration. The percentage of inhibition was calculated and the results were expressed in Trolox equivalents. Total antioxidant activity is defined in terms of the concentration of Trolox that has equivalent antioxidant activity and is expressed in µmol/g sample.

Hydrogen peroxide scavenging activity

The ability of Ag-NPs to scavenge hydrogen peroxide (H_2O_2) was determined according to the method of Ruch et al.[28] A solution of H_2O_2 (2 µmol/L) was prepared in phosphate buffer (0.2 M, pH 7.4) and its concentration was determined spectrophotometrically at 230 nm with molar absorptivity of 81 M^{-1}/cm. An Ag-NP-suspended solution (10 µL) was added to 3.4 mL of phosphate buffer together with 0.6 mL of H_2O_2. An identical reaction mixture without the sample was used as a negative control. Absorbance of H_2O_2 at 230 nm was determined after 10 minutes against the blank solution (phosphate buffer). The scavenging activity (in percentage) was calculated according to the following formula: scavenging activity (%) = $[(A_0 - A_1)/A_0] \times 100$, where A_0 is the absorbance of the control (reaction mixture without sample) and A_1 is the absorbance of the sample/standard.

In vitro antimicrobial activity

Microbial cultures

Both bacterial and fungal strains were collected from the Microbial Type Culture Collection (MTCC), Institute of Microbial Technology, Chandigarh, India. The bacterial

strains included the gram-positive bacteria, *Bacillus subtilis* Ehrenberg (MTCC 441), *Bacillus cereus* Bizio (MTCC 1272), and *Bacillus megaterium* A. deBary (MTCC 2444), as well as the gram-negative bacterial strains, *Escherichia coli* Escherich (MTCC 1195), *Proteus vulgaris* Hauser (MTCC 1771), *Serratia marcescens* Bizio (MTCC 8780), *Salmonella typhi* Eberth (MTCC 733), *Klebsiella pneumoniae* Friedlander (MTCC 2405), *Vibrio cholerae* Pacini (MTCC 3904), *Shigella sonnei* Carl Olaf Sonne (MTCC 2957), *Enterobacter aerogenes* Bizio (MTCC 2823), and *Pseudomonas aeruginosa* Schroeter (MTCC 2642). The fungal strains including *Aspergillus niger* van Tieghem (MTCC 2425), *Aspergillus flavus* Link ex-Gray (MTCC 3396), *Fusarium oxysporum* Schlecht (MTCC 2480), *Penicillium chrysogenum* Thom. (MTCC 2725), and *Rhizopus oryzae* Went & Prins. Geerl. (MTCC 262) were selected for antifungal assays.

Antimicrobial assays

The antimicrobial activities of biosynthesized Ag-NPs, $AgNO_3$, and standard antibiotic (chloramphenicol) were examined using three different assays: a disk diffusion assay for both antibacterial and antifungal activities, a time-course growth assay, and a minimum inhibitory concentration (MIC) assay.

Antibacterial disk diffusion assay

Agar plates were made by pouring 20 mL of sterile nutrient agar liquid medium (pH 7.4±0.2) into sterile Petri plates. After solidification, 100 µL of suspension, containing 10^5 colony forming units/mL of each bacterial sample, was spread over the nutrient agar plates. Sterile filter paper disks (6 mm in diameter) were impregnated with 5 and 10 mg/mL of $AgNO_3$ and Ag-NP suspended solution, respectively. Sample-loaded disks were placed on the inoculated agar plates. Chloramphenicol (10 mg/mL) was used as a positive reference control to determine the sensitivity of each bacterial species to Ag-NPs. The inoculated plates were incubated at 37°C for 24 hours. Antibacterial activity was evaluated by measuring zones of inhibition against the test organisms. Each assay contained three technical replicates.[29]

Antifungal disk diffusion assay

The antifungal activity of biosynthesized Ag-NPs and $AgNO_3$ was tested using disk diffusion.[30] Potato dextrose agar plates were inoculated with fungal cultures (10 days old) by point inoculation. Filter paper disks (Whatman No 1, 6 mm diameter) were impregnated with 5 and 10 mg/mL $AgNO_3$ and Ag-NPs, respectively, and were then placed on test organism-seeded plates. Nystatin (10 mg/mL) was used as positive control. Activity was determined after 72 hours of incubation at 28°C. Diameters of inhibition zones were measured with a caliper and their mean values were calculated.

Time course growth assay

A time course growth assay was used to evaluate the antibacterial sensitivity of pathogenic bacterial strains to Ag-NPs and $AgNO_3$ through time. One hundred microliters of overnight bacterial culture in nutrient broth (NA) was added to sterile test tubes containing 1 mL of NA containing 100 µL of 5 and 10 mg/mL $AgNO_3$ and Ag-NPs, respectively. The inoculated tubes were incubated at 37°C after shaking. Optical density at 550 nm was measured using a microquant spectrophotometer (BioTek, USA) after 0, 1, 2, 3, and 5 hours. A decrease in optical density was observed in the incubated cultures, suggesting a bacteriostatic effect.[31] Each assay contained three technical replicates.

Minimum inhibitory concentration

Different concentrations of samples were tested for the MIC required to affect bacterial growth. Three milliliters of NA, 0.1 mL of bacterial suspension, and $AgNO_3$ and Ag-NPs (5 and 10 mg/mL, respectively) suspended in double-distilled water were added to each test tube. Tubes were incubated at 37°C for 24 hours. After 24 hours, turbidity in each test tube was measured using a spectrophotometer at 420 nm. This turbidity measurement was taken as an indicator of the bacterial density, and the relationship between this and the sample inhibition rate was assessed.[32]

In vivo anti-inflammatory activity

Animals

Female Wistar albino rats (120–150 g) were used throughout the experimental study, and were housed in polypropylene cages with sterile husk materials. The experimental animals were maintained under controlled environmental conditions at 23°C±2°C and a relative humidity of 55%±10% on a 12-hour light/dark cycle. The experimental rats were allowed to acclimatize for 1 week prior to experimentation, and were thereafter provided with water and the standard pellet diet.

Ethics

The animal experimental protocols used in this study were approved by the Institutional Animal Care and Use Committee of Sri Krishnadevaraya University at Anantapur, Andhra Pradesh, India (Reg No 25/1/99/AWD) and followed the national guidelines of India for animal care.

Acute toxicity

According to the Organization for Economic Cooperation and Department, acute oral toxicity studies were carried out by random sampling technique.[33] Six Wistar albino adult female rats were then selected for the study; these were fasted for 12 hours with free access to water. Ag-NPs suspended in hydrosol were orally administered at a dose of 5 mg/kg for 3 days and their effects on rat mortality were observed. If mortality was observed in more than four of six animals, then the dose administered was considered as toxic dose. Furthermore, if mortality was observed in only one of six animals, then the study was repeated with a higher dose. The higher doses used were 25, 50, 75, and 100 mg/kg. General behaviors such as motor activity, tremors, convulsions, Straub reaction, aggressiveness, piloerection, loss of righting reflex, sedation, muscle relaxation, hypnosis, analgesia, ptosis, lacrimation, diarrhea, and skin color were observed for the first 1 hour and then 24 hours after drug administration.

Anti-inflammatory activity

The in vivo anti-inflammatory activity of biosynthesized Ag-NPs was evaluated in Wistar albino adult female rats using the standard carrageenan-induced paw edema method.[34] The animals were divided into five different groups with each group containing six rats. The animals were fasted overnight with free access to water before treatment. Group I rats (positive control) received water alone. Group II (negative control) rats were treated with carrageenan (10 mg/kg; Hi-Media, Mumbai, India) to induce inflammation. Group III animals were treated with indomethacin (10 mg/kg) as the standard drug. Group IV and V rats were treated with 50 and 100 mg/kg of biosynthesized Ag-NPs, respectively. Indomethacin and biosynthesized Ag-NPs were administered orally 30 minutes before the administration of carrageenan in the right hind paws of experimental rats. Finally, paw volume was measured using a Plethysmometer (Plethysmometer (Panlab, LE7500, USA) at intervals of 0, 1, 2, 3, and 24 hours to study the in vivo anti-inflammatory activity of Ag-NPs. The percentage of inhibition of paw edema was calculated by the following formula:

$$\text{Percentage of inhibition} = \frac{V_c - V_t}{V_c} \times 100$$

where V_t is the increase in paw volume of rats treated with the sample drug and V_c is the increase in paw volume of the positive control group.

Statistical analysis

All experiments were performed with groups of six animals each and the results were expressed as mean ± the standard error of mean. All data were analyzed using Statistical Package for the Social Sciences 17.0 software (SPSS Inc., Chicago, IL, USA) with one-way analyses of variance followed by Duncan's new multiple range test (DMRT), with an alpha level of 0.05.

Results and discussion

Biosynthesis of Ag-NPs

Biosynthesis of Ag-NPs from $AgNO_3$ is one of the most widely used methods for silver colloid synthesis. The biosynthesized Ag-NPs were characterized using UV–vis spectrophotometry, FTIR, EDAX, SEM, and HRTEM. The ability of the plant leaf extract to reduce silver ions to Ag-NPs was confirmed by the reddish-brown color change in the reaction mixture.

UV–vis spectrum analysis

For the synthesis of Ag-NPs, the reaction mixture contained an aqueous leaf extract of *P. tripartita* Sw. and an aqueous solution of $AgNO_3$ (1 M). This solution, which was initially colorless, turned reddish-brown, indicating the synthesis of Ag-NPs by the reduction of silver ions in solution. Their characteristic surface plasmon absorption was observed at 428 nm; this was very close to the surface plasmon resonance wavelength of silver (Figure 1A). The surface plasmon resonance of Ag-NPs depends on both the size and shape of particles, and several investigators have already reported the absorption of colloidal silver solution between 410 and 440 nm.[35–40] The reddish-brown color change occurs due to excitation of the surface plasmon vibration of the metal NPs.

FTIR analysis

FTIR absorption spectra revealed the functional groups involved in the bioreduction of NPs. Aqueous extracts of *P. tripartita* Sw. contain numerous bioactive compounds including phenolics, flavonoids, terpenoids, tannins, proteins, and glycosides. Of these compounds, flavonoids play a vital role as reducing agents during NP synthesis. FTIR spectra were recorded for biosynthesized Ag-NPs produced from aqueous leaf extracts using a Spectrum 100 spectrometer (PerkinElmer Inc.). Spectra were observed in the range of 650–4,000 cm^{-1} (mid-infrared). The FTIR spectrum of the reddish-brown suspension showed four different peaks at 3,416, 2,082, 1,639, and 672 cm^{-1}, respectively (Figure 1B). The broad band at 3,416 cm^{-1} (–OH or –NH) showed the presence of hydrogen bonded hydroxyl (–OH)

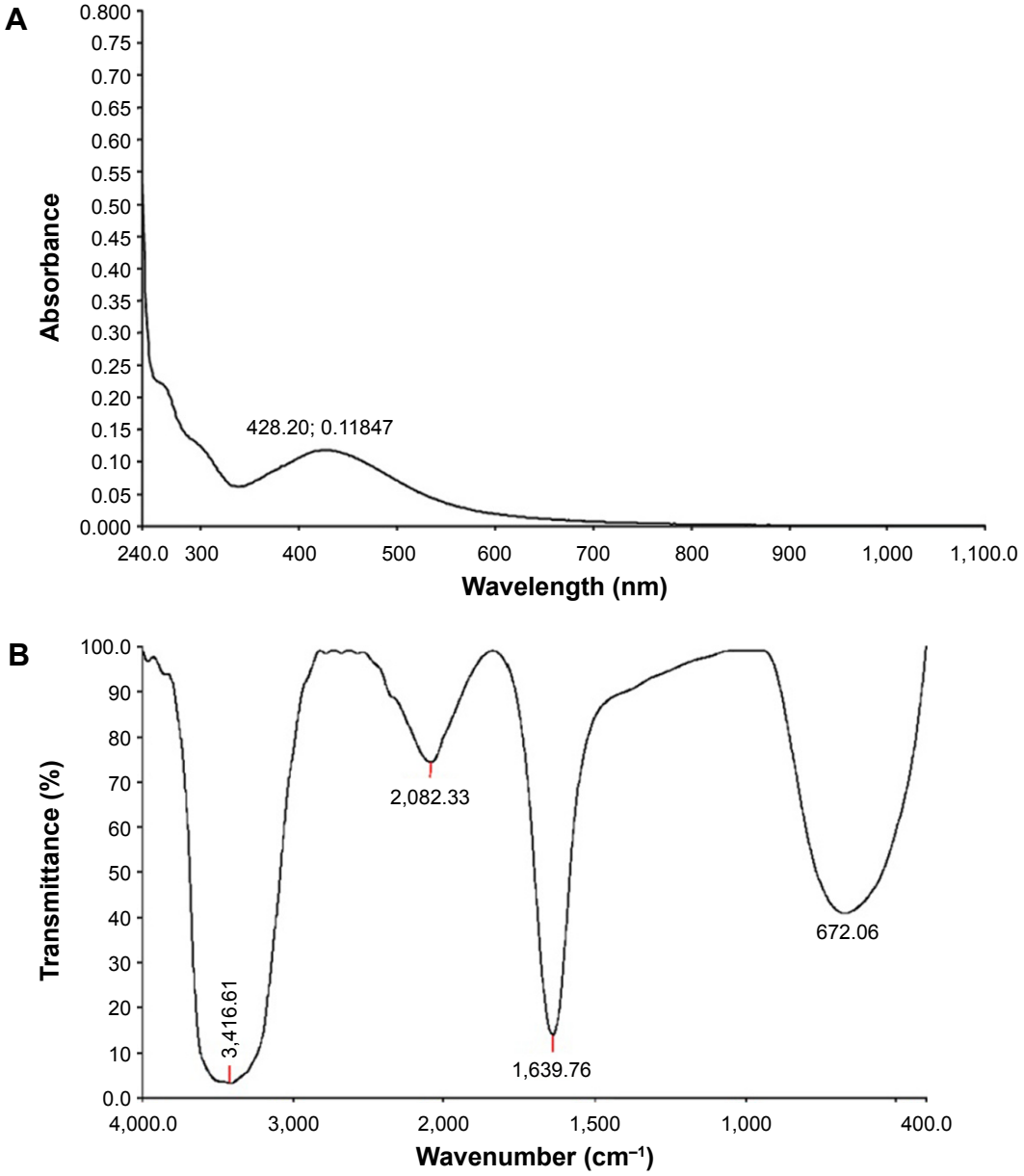

Figure 1 (**A**) UV-visible spectra and (**B**) FTIR spectra of Ag-NPs synthesized using *Pteris tripartita* Sw. leaf extract with 1 M $AgNO_3$ solution.
Abbreviations: $AgNO_3$, silver nitrate; Ag-NPs, silver nanoparticles; FTIR, Fourier transform infrared spectroscopy; UV, ultraviolet.

group compounds. The "hydrogen region", which ranges from 3,800 to 2,700 cm^{-1}, is the highest energy region of the spectrum, and spectra in the range from 3,200 to 3,400 cm^{-1} may indicate alcohols, carbohydrates, and phenols. A sharp band at 1,639.76 cm^{-1} showed C=O stretching bonds of the carbonyl group, and the absorption peak near 1,700 cm^{-1} indicated the presence of aldehyde, ketone, carboxylic acids, and amide (I, II, III) group compounds. The carbonyl group of amino acid residues has the ability to strongly bind metals. Proteins containing these residues may form a coat which covers metal NPs and prevents the particles from forming agglomerations in solution.[41] The capping ligand of Ag-NPs may have an aromatic compound, alkane, or amine.[42] The wide absorption spectra at 1,635 cm^{-1} might result from the stretch vibrations of –C=C, which was also observed in an earlier study.[43] Tian et al[44] reported that isolated flavonoids, namely, quercetin and quercetin 3-*O*-glycosides from lotus leaves, were also used in Ag-NP synthesis. According to Baskaran,[21] high-performance liquid chromatography analysis of an ethanol extract of *P. tripartita* Sw. showed the presence of flavonoids, including quercetin and rutin. Furthermore, metabolites such as reducing sugars and terpenoids found in neem leaf broth are believed to be the surface-active molecules that stabilize NPs.[11] An extract

of *Capsicum annuum* revealed the role played by individual residues within proteins in the reduction of silver ions to Ag-NPs.[45] Moreover, secondary metabolites like alkaloids, flavonoids, tannins, and cardiac glycosides, which were all present in the extract of *Tagetes erecta*, may have been responsible for stabilizing the synthesized NPs in an earlier study.[23] Thus, these FTIR spectra confirmed the production of Ag-NPs by the reduction of Ag^+ ions due to the capping material of *P. tripartita* aqueous leaf extract.

EDAX analysis

EDAX spectra of Ag-NPs were recorded and are shown in Figure 2. EDAX spectra of Ag-NPs showed a strong signal for silver atoms, as well as weaker signals for O and Cl atoms. The bonds might be due to biomolecules of plant extract being bound on the surface of Ag-NPs. A similar result was also observed in biosynthesized Ag-NPs derived from *Magnolia kobus* broth.[22] Our results agree with these studies, and, in the present study, Ag-NP biosynthesized from *P. tripartita* seems to be relatively chemically pure.[46] EDAX spectra confirmed the presence of Ag-NPs as evidenced by strong signal energy peaks for silver atoms in the range of 2–4 keV. By using a similar isolation protocol, Gardea-Torresdey et al[15] obtained individual spherical Ag-NPs in the range of 2.5–4 keV using alfalfa broth.

SEM and HRTEM analysis of Ag-NPs

Using a SEM, we observed a high density of Ag-NPs in solid phase; these images are given in Figure 3A and B. SEM data, produced at different magnifications, revealed biosynthesized Ag-NPs between 10 and 50 µm. HRTEM analysis revealed that Ag-NPs in liquid phase existed in a range of sizes, including 4, 10, 11, 13.4, 14, 27.5, 30, 39, and 43 nm. Ag-NP morphology was also variable; different shapes were observed, including hexagons, spheres, and rod shapes. HRTEM images of biosynthesized Ag-NPs are given in Figure 3C and D.

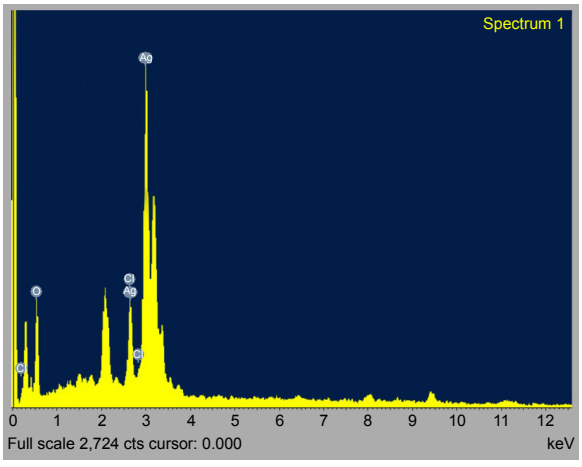

Figure 2 EDAX spectrum of Ag-NPs biosynthesized using *Pteris tripartita* Sw. leaf extract.
Abbreviations: Ag-NPs, silver nanoparticles; EDAX, energy-dispersive X-ray analysis.

XRD analysis for Ag-NPs

The crystalline structure of Ag-NPs was confirmed using XRD. This technique is commonly used to estimate the sizes of NPs in the range 1–100 nm. We observed strong peaks, indicating a high degree of crystallinity of biosynthesized Ag-NPs. We observed Bragg's angle (2θ) values of 35.1°, 37.8°, 38.7°, and 53.4°, which correspond to values of (100), (101), (102), and (104) for the crystal reflection planes of the face-centered cubic (fcc) crystal structure of silver (Joint Committee on Powder Diffraction Standards data no 87-0598) (Figure 4). A sharp, intense peak was observed at 35.1° among 2θ values. The crystalline domain sizes of Ag-NPs were calculated from the widths of XRD peaks using Scherrer's formula: $D = 0.94\,\lambda/\beta \cos\theta$, where D represents the average crystalline domain size perpendicular to the reflecting planes, λ the X-ray wavelength, β the full width at half maximum, and θ represents the diffraction angle. The slight discrepancy in particle size calculation by XRD and HRTEM measurements can be attributed to experimental error, due to the use of bulk amounts of sample in the XRD measurements. Silver nanocrystallite size at maximum intensity (100%) was estimated using Scherrer's formula, where the crystallite peak was 32 nm. The sizes of Ag-NPs synthesized from *P. tripartita* are given in Table 1. In earlier studies, the same pattern of diffraction was observed at 31.76°, 31.90°, 32.16°, 32.20°, 32.21°, 38.09°, 35.10°, 37.60°, 38.06°, and 54.75° for biosynthesized Ag-NPs.[42,47–52] In addition, the observed XRD patterns for Ag-NPs synthesized from *Trianthema decandra* and *Sesuvium portulacastrum* extracts showed three intense peaks ranging from 10 to 80.[53,54]

In vitro antioxidant activities

DPPH· is a stable nitrogen-centered free radical that changes its color from violet to yellow upon reduction – accepting hydrogen or donating an electron.[55] For this reason, the lowest IC_{50} value identifies the strongest level of antioxidant activity. In the present study, biosynthesized Ag-NPs showed relatively high antioxidant activity (47.90 µg/mL) (Table 2). In an earlier study, a water-based extract of *P. tripartita* showed comparatively less activity (116.27 µg/mL) than did *P. tripartita* Ag-NPs.[20] The IC_{50} values of standard

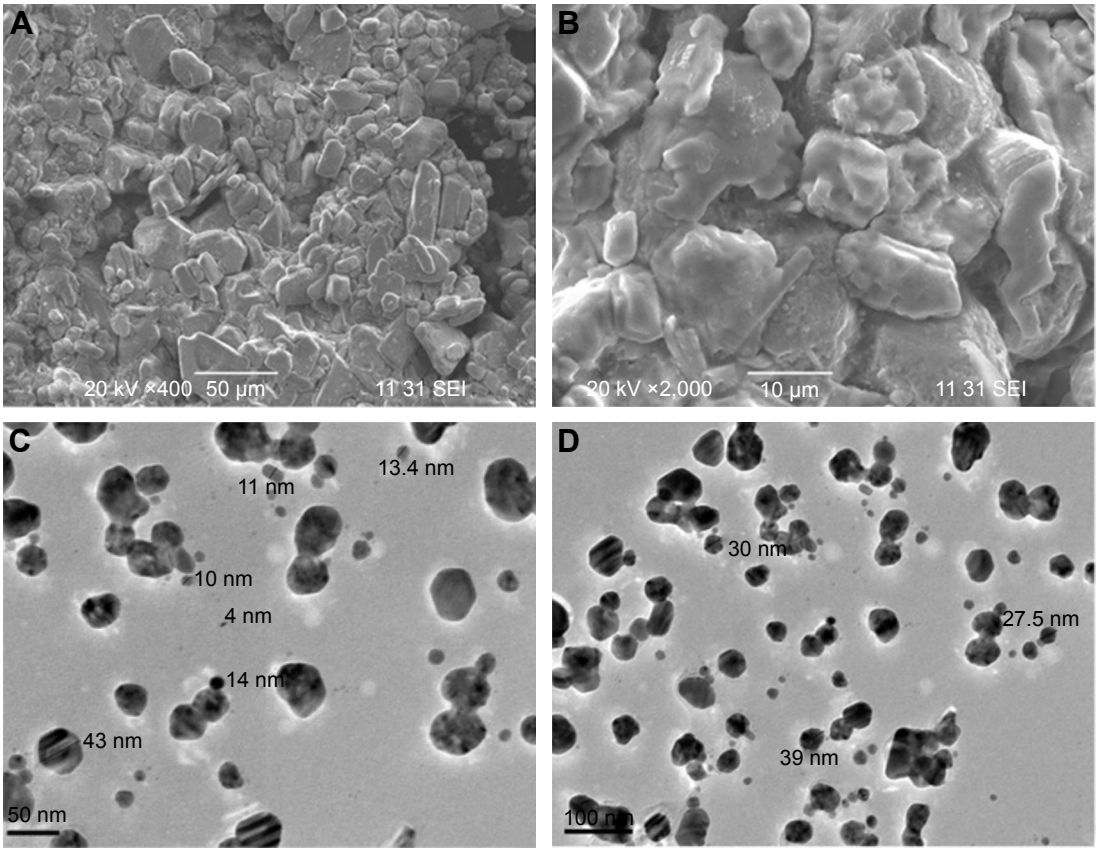

Figure 3 SEM (**A**, **B**) and HRTEM (**C**, **D**) images of silver nanoparticles biosynthesized using *Pteris tripartita* Sw. leaf extract.
Abbreviations: HRTEM, high-resolution transmission electron microscopy; SEM, scanning electron microscopy; SEI, secondary electron image.

antioxidants were found to significantly differ from those of biosynthesized NPs. In earlier studies, Ag-NPs exhibited both significant scavenging of DPPH, H_2O_2, and ABTS, as well as significant metal chelating activity.[56–63]

Iron is an important catalyst of lipid oxidation and a pro-oxidant due to its high reactivity. In the ferrous state, iron accelerates lipid oxidation by breaking down hydrogen and lipid peroxides to reactive free radicals. Ferrozine can quantitatively form complexes with Fe^{2+}, and their complex formation is disrupted by the presence of other chelating agents. The measurement of specific OD values helps to estimate the metal chelating activity.[64] The metal chelating effects of biosynthesized Ag-NPs are shown in Table 2. Biosynthesized Ag-NPs showed the highest metal chelating activity (61.51 µg EDTA/g). We conclude that chelating agents act as secondary antioxidants, which reduce the redox potential and stabilize the oxidized forms of metal ions.[65] In contrast, the water extract of *P. tripartita* displayed the lowest metal chelating activity (9.22 µg EDTA/g).[20] The quantitative antioxidant capacity of biosynthesized Ag-NPs was measured using a phosphomolybdenum assay; this technique measures the reduction of Mo (VI) to Mo (V) by antioxidant compounds. The reducing activity is indicated by the formation of green phosphate/Mo (V) complex, which has maximal absorption at 695 nm. Biosynthesized Ag-NPs showed 41.94 mg AAE/g of phosphomolybdenum reduction activity in the present study, and the water extract had the lowest activity (21.26 mg AAE/g).[20] It should be noted that

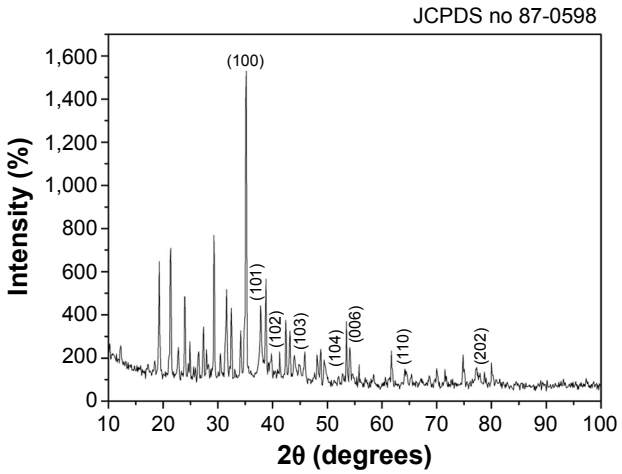

Figure 4 XRD pattern for Ag-NPs synthesized from *Pteris tripartita* aqueous leaves.
Abbreviations: Ag-NPs, silver nanoparticles; XRD, X-ray diffraction; JCPDS, Joint Committee on Powder Diffraction Standards.

Table 1 Various sizes of Ag-NPs by *Pteris tripartita* Sw. using Scherrer's equation

Serial no	2θ (°)	D (ang)	I	FWHM (°)	I (counts)	Integrated I (counts)	Size (nm)
1	19.2806	4.59984	32	0.28250	210	650	28
2	21.3514	4.15817	40	0.28440	262	868	28
3	23.9408	3.71397	26	0.24970	169	446	32
4	29.3140	3.04428	44	0.24910	288	800	33
5	31.5173	2.83630	25	0.37910	166	691	22
6	32.4539	2.75656	21	0.26470	139	417	31
7	35.1293	2.55251	100	0.26180	662	1,944	32
8	37.8073	2.37763	24	0.36990	157	633	23
9	38.7526	2.32178	29	0.28880	192	656	29
10	53.4861	1.71182	19	0.21880	128	301	41

Abbreviations: Ag-NPs, silver nanoparticles; FWHM, full width at half maximum; S, serial number; I, intensity.

electron transfer occurs at different redox potentials in the ferrozine and phosphomolybdenum assays, and in each case, the reducing activity depends on the structure of the antioxidant under study.[66]

Another technique, the $ABTS^{\cdot+}$ assay, is an excellent tool to determine the antioxidant activity of hydrogen-donating antioxidants (scavenging aqueous phase radicals) and of chain-breaking antioxidants (scavenging lipid peroxyl radicals). Biosynthesized Ag-NPs showed significant antioxidant activity (8,592.70 µmol Trolox/g), while the water extract did not (920.69 µmol Trolox/g; unpublished data). In an H_2O_2 assay, biosynthesized Ag-NPs showed 16.20% inhibition, whereas the water extract showed 26.18% inhibition (unpublished data). In all assays included in the present study, with the exception of H_2O_2 assay, biosynthesized Ag-NPs exhibited highest antioxidant activity and prove the discrepancy in the activities of NPs and plant extracts.

In vitro antimicrobial activity

Disk diffusion antibacterial assay

Significant inhibition of both gram-positive and gram-negative bacterial strains was observed. The diameter of inhibitory zones ranged from 7.66 to 38.33 mm for $AgNO_3$ and Ag-NPs treatments, respectively (Table 3; Figure 5). The highest inhibitory effect was observed in treatment with 10 mg of $AgNO_3$ against *P. aeruginosa* (38.33 mm), followed by 5 mg of $AgNO_3$ (23 mm), 5 mg of Ag-NPs (24.3 mm), and 10 mg of Ag-NPs (23 mm), respectively. Moderate inhibitory zones were observed with both $AgNO_3$ and Ag-NP treatments against bacterial strains. Of them, 5 mg of $AgNO_3$ showed inhibition zones ranging from 10.66 to 23.00 mm. Furthermore, treatment with 10 mg of Ag-NP showed inhibitory zones against *P. vulgaris* (19.33 mm), *S. typhi* (16.33 mm), *V. cholerae* (15.33 mm), *S. sonnei* (11.00 mm), *K. pneumoniae* (15.66 mm), *E. aerogenes* (11.33 mm), and *B. megaterium* (11.66 mm). The minimum inhibition zones were noticed against *B. subtilis* (9 mm), *E. coli*, and *B. cereus* (8.33 mm), despite the fact that Prasad et al[35] reported that biosynthesized Ag-NPs showed antimicrobial activity against *E. coli*, *K. pneumoniae*, and *B. cereus*. Previous studies have also reported that Ag-NPs exhibited antibactericidal effects against *S. aureus*, *Pseudomonas* sp. and *E. coli*.[67–71] In addition, biosynthesized Ag-NPs isolated from *Citrullus colocynthis* callus and *Phyllanthus amarus* extracts exhibited tremendous antibacterial activity against *E. coli*, *P. aeruginosa*, and *P. vulgaris*.[5,52] Both the concentrations of Ag-NPs (5 and 10 mg/mL) did not show any inhibitory activity against *S. marcescens* and positive strains like *B. cereus*

Table 2 In vitro antioxidant activities of biosynthesized Ag-NPs and standard flavonoids

Samples	DPPH assay (µg/mL)	Metal chelating activity (mg EDTA/g)	Phosphomolybdenum assay (mg AAE/g)	$ABTS^{\cdot+}$ assay (µmol Trolox/g)	H_2O_2 assay (%)
Ag-NPs	47.90	61.51±0.61	41.94±2.29	8,592.70±614.2	16.20±3.86
Quercetin	18.79	17.99±0.04	100.35±3.34	60,074.65±380.34	62.22±1.74
Rutin	24.71	18.13±0.04	148.77±3.34	15,403.41±235.37	57.84±5.04
BHA	25.58	–	–	–	
BHT	45.56	–	–	–	

Notes: All values are expressed as mean ± SE and analyzed using SPSS 17.0 software (SPSS Inc., Chicago, IL, USA) with one-way ANOVA followed by DMRT and their relationship was considered to be statistically significant when $P<0.05$. In DPPH assay, mean values calculated in Microsoft Excel 2007.

Abbreviations: AAE, ascorbic acid equivalents; ABTS, azinobis 3-ethylbenzothiazoline-6-sulfonate; Ag-NPs, silver nanoparticles; ANOVA, analysis of variance; BHA, butylated hydroxyanisole; BHT, butylated hydroxytoluene; DMRT, Duncan's new multiple range test; EDTA, ethylenediaminetetraacetic acid; SE, standard error; SPSS, Statistical Package for the Social Sciences.

Table 3 Antimicrobial activity of $AgNO_3$, biosynthesized Ag-NPs, and standard antibiotics against different pathogens

Microorganisms	$AgNO_3$ 5 mg/mL	$AgNO_3$ 10 mg/mL	Ag-NPs 5 mg/mL	Ag-NPs 10 mg/mL	Standard antibiotics
Bacteria (mm)					Chloramphenicol (10 mg/mL)
Bacillus cereus	7.66±0.33	9.00±0.57	–	8.33±0.33	33.66±2.18
Bacillus subtilis	–	–	–	9.00±0.57	33.33±0.66
Bacillus megaterium	9.66±0.33	8.66±0.33	9.00±0.57	11.66±0.88	24.66±2.02
Shigella sonnei	–	16.33±1.33	11.00±1.00	13.33±1.20	28.00±0.00
Vibrio cholerae	10.66±0.33	15.66±0.66	12.66±2.18	15.33±0.33	25.66±0.66
Pseudomonas aeruginosa	23.00±0.57	38.33±0.33	23.00±0.57	24.33±0.66	28.66±0.33
Klebsiella pneumoniae	15.66±0.33	16.33±0.66	14.66±0.33	15.66±0.33	24.00±0.57
Serratia marcescens	9.66±0.66	11.00±0.57	–	–	31.00±2.08
Escherichia coli	11.00±0.57	7.66±0.66	10.33±0.33	8.33±0.66	26.33±0.88
Enterobacter aerogenes	9.66±0.33	11.33±0.33	10.00±0.00	11.33±0.66	26.00±1.00
Salmonella typhi	11.33±0.33	16.00±1.00	13.33±1.66	16.33±1.20	29.33±1.76
Proteus vulgaris	16.66±0.33	19.33±0.66	13.33±1.45	19.33±1.20	30.00±0.00
Fungi (mm)					Nystatin (10 mg/mL)
Aspergillus niger	11.66±0.61	16.33±0.33	15.33±0.66	–	16.36±0.37
Aspergillus Flavus	15.66±0.66	17.66±1.45	13.33±0.88	15.33±0.33	14.70±0.51
Fusarium oxysporum	12.00±0.00	12.00±0.57	12.66±0.33	13.66±0.66	14.23±0.34
Penicillium chrysogenum	–	–	12.66±0.66	–	18.80±0.20
Rizopus oryzae	13.66±0.33	12.66±0.66	15.00±0.57	14.66±0.66	13.90±0.40

Notes: All values represented as mean ± SE of triplicate values and analyzed using SPSS 17.0 software with one-way ANOVA followed by DMRT and their relationship was considered to be statistically significant when $P<0.05$.

Abbreviations: $AgNO_3$, silver nitrate; Ag-NPs, silver nanoparticles; ANOVA, analysis of variance; DMRT, Duncan's new multiple range test; SE, standard error; SPSS, Statistical Package for the Social Sciences.

and *B. subtilis*. Moreover, the Ag-NP treatment (5 mg/mL) exhibited an inhibition zone of 24.33 mm, while the positive control showed a zone of 28.66 mm against *P. aeruginosa*. The positive control, chloramphenicol, showed an inhibitory zone against all bacterial strains, ranging from 24.00 to 33.66 mm. However, significant inhibitory zones ranging from 23.00 to 38.33 mm were observed against *P. aeruginosa*.

Disk diffusion antifungal assay

Table 3 summarizes the antifungal activity of Ag-NPs, which was again measured by the diameter of inhibition zones. $AgNO_3$ (5 mg/mL) and Ag-NP treatments showed significant antifungal activities against *A. niger* (16.33 mm), *A. flavus* (17.66 mm), *F. oxysporum* (12 mm), and *R. oryzae* (12.66 mm) (Figure 6). Treatment with $AgNO_3$ (5 mg/mL) formed an inhibitory zone of 15.66 mm against *A. flavus*, of 12.00 mm against *F. oxysporum*, and of 13.66 mm against *R. oryzae*. Panacek et al[72] reported that Ag-NPs possessed antifungal properties because extracellular synthesis of NP helps trap metal ions on the cell surface and helps reduce ions in the presence of enzymes. In earlier studies, Ag-NPs showed biological activity against fungal strains.[14,35,72,73]

Time course growth assay

The Ag-NPs strongly inhibited the growth of eleven different bacterial strains; for example, treatment with 5 mg/mL Ag-NP showed an OD of 0.26 against *P. vulgaris*, and of 0.29 OD against *E. aerogenes* (Table 4). However, treatment with the stronger 10 mg/mL Ag-NP showed significant inhibition against *P. vulgaris* (0.27 OD), *K. pneumoniae* (0.29 OD), *E. aerogenes* (0.28 OD), and *B. megaterium* (0.26 OD). The positive control (chloramphenicol) inhibited all the bacterial strains and showed optical density values ranging from 0.11 to 0.46. Previous studies have found that Ag-NPs inactivate microbes by interacting with their enzymes, proteins, or DNA, and thereby inhibit cell proliferation.[11]

Minimum inhibitory concentration

We assessed the MIC values of $AgNO_3$, Ag-NPs, and chloramphenicol against 12 bacterial strains by using the microdilution technique with 96-well microtiter plates (Table 4). Generally, the MIC values are interpreted as the lowest concentration that inhibits visible microbial growth and are expressed in terms of mg/mL.[74] Since the 19th century, dilute solutions of $AgNO_3$ have been used to treat infections and burns. Most probably, the antibacterial activities of this solution are derived from an electrostatic attraction between the negatively charged cell membrane of a microorganism and the positively charged NPs.[75]

Although somewhat similar, the bioactivity of Ag-NPs against pathogens was found to be size- and dose-dependent, and also exhibited more pronounced activity against

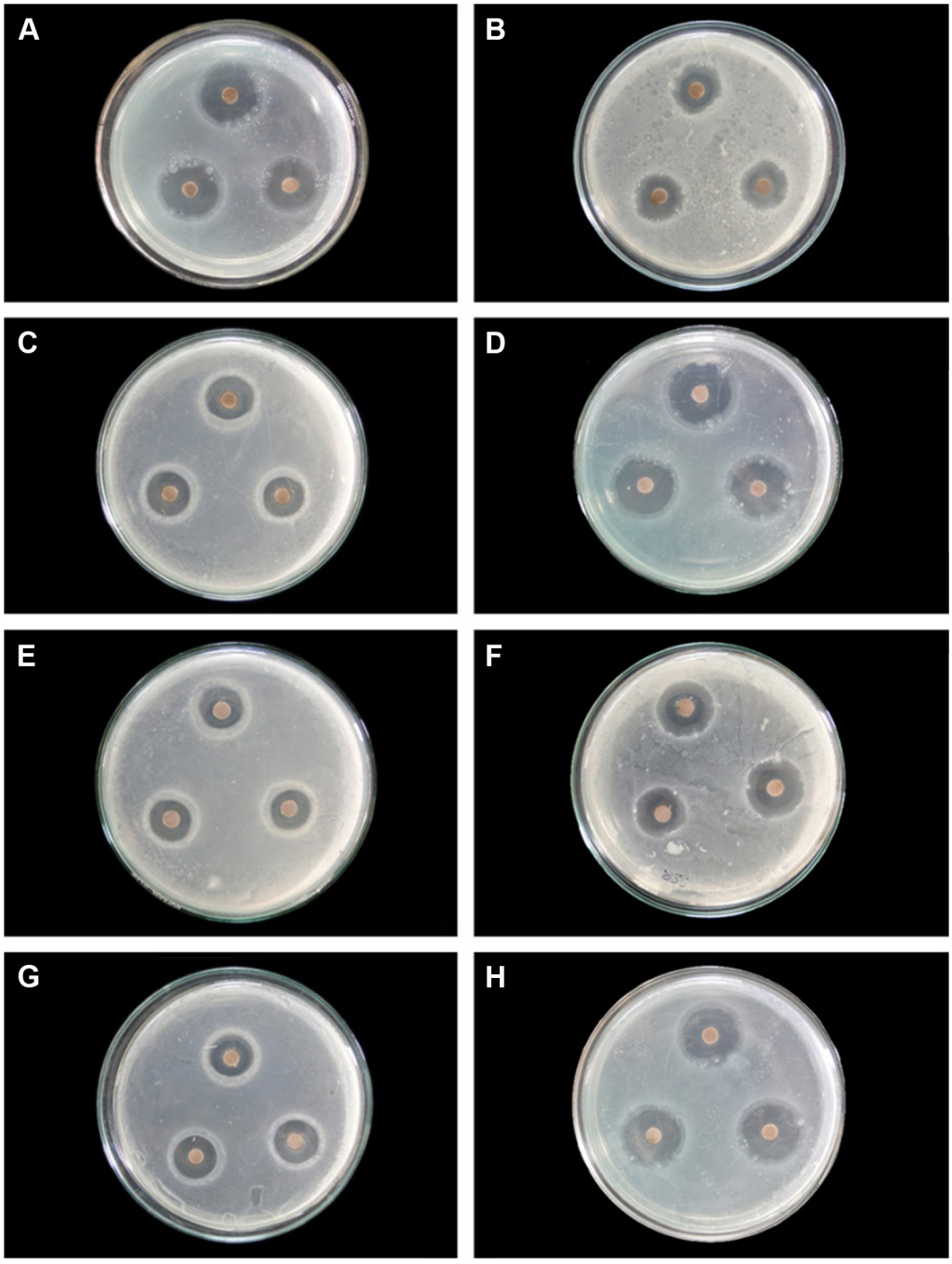

Figure 5 Antibacterial activity of $AgNO_3$ and biosynthesized Ag-NPs.
Notes: (**A**) *Pseudomonas aeruginosa* (5 mg/mL of $AgNO_3$), (**B**) *Proteus vulgaris* (10 mg/mL of $AgNO_3$), (**C**) *Klebsiella pneumoniae* (10 mg/mL of $AgNO_3$), (**D**) *P. aeruginosa* (5 mg/mL of Ag-NPs), (**E**) *K. pneumoniae* (5 mg/mL of Ag-NPs), (**F**) *P. vulgaris* (10 mg/mL of Ag-NPs), (**G**) *K. pneumoniae* (10 mg/mL of Ag-NPs), (**H**) *P. aeruginosa* (10 mg/mL of Ag-NPs).
Abbreviations: $AgNO_3$, silver nitrate; Ag-NPs, silver nanoparticles.

gram-negative bacteria than gram-positive bacteria.[70,76] In an earlier study, Ag-NPs revealed significant activity against pathogens.[77] Treatment with 5 mg/mL $AgNO_3$ showed significant MIC values against *P. aeruginosa* (0.98 OD), *K. pneumoniae* (0.92 OD), *E. aerogenes* (0.19 OD), *B. cereus* (0.24 OD), and *B. megaterium* (0.18 OD). In contrast, treatment with 10 mg/mL $AgNO_3$ inhibited *S. typhi* (0.73 OD), *P. vulgaris* (0.60 OD), *S. sonnei* (0.68 OD), *P. aeruginosa* (0.92 OD), *K. pneumoniae* (0.72 OD), *S. marcescens* (0.99 OD), and *B. cereus* (0.43 OD), respectively. However, treatment with 10 mg/mL $AgNO_3$ showed a markedly lower MIC value against *B. cereus* (0.43 OD). The antibacterial activity of

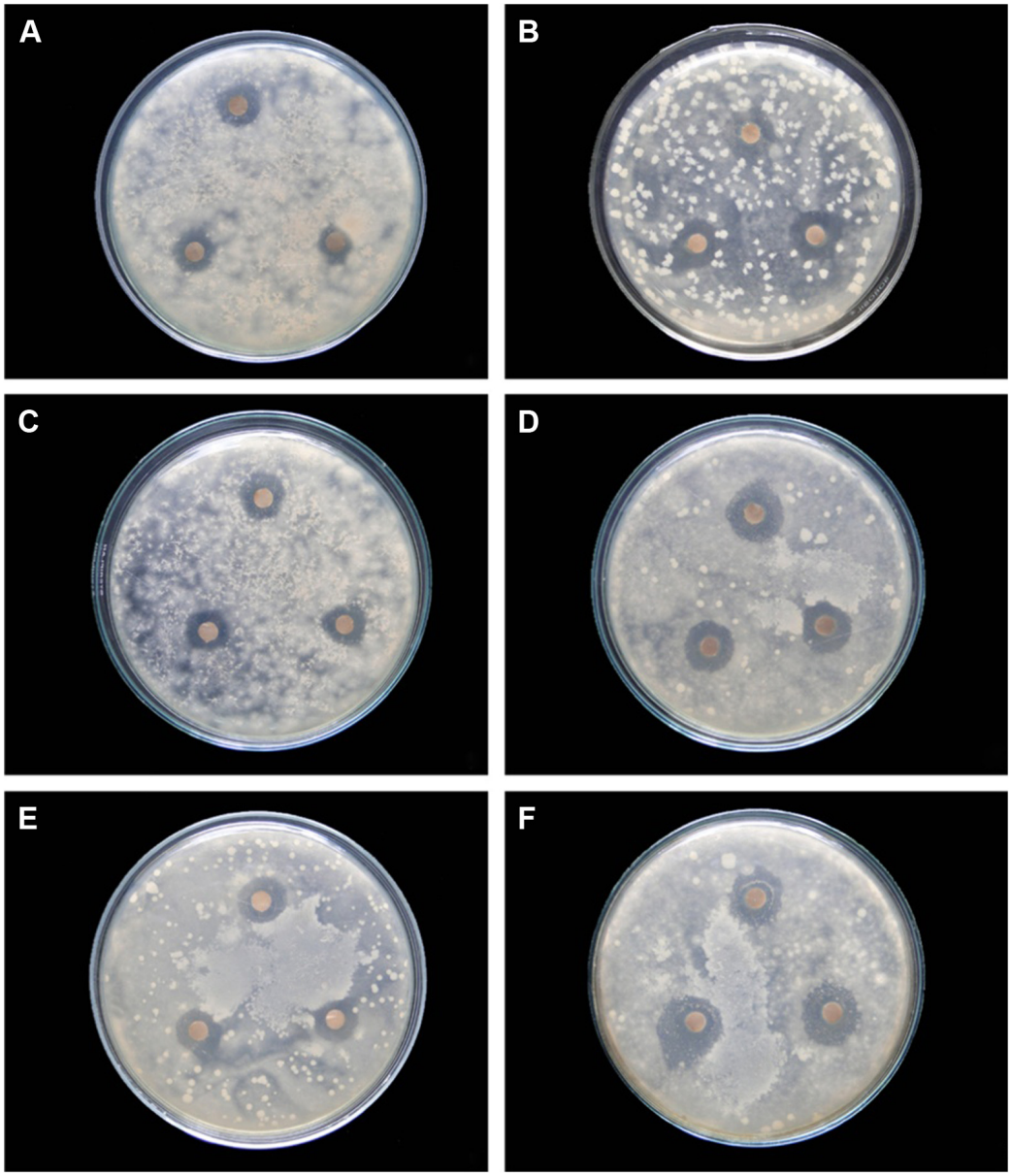

Figure 6 Antifungal activity of $AgNO_3$ and biosynthesized Ag-NPs.
Notes: (**A**) *Aspergillus flavus* (5 mg/mL of Ag-NPs), (**B**) *Fusarium oxysporum* (5 mg/mL of Ag-NPs), (**C**) *Penicillium chrysogenum* (5 mg/mL of Ag-NPs), (**D**) *A. flavus* (5 mg/mL of $AgNO_3$), (**E**) *Rhizopus oryzae* (10 mg/mL of $AgNO_3$), (**F**) *A. flavus* (10 mg/mL of $AgNO_3$).
Abbreviations: $AgNO_3$, silver nitrate; Ag-NPs, silver nanoparticles.

Ag-NPs has been well documented in previous studies,[52,78,79] likely because larger specific surface area yields improved antimicrobial activity.[80] The mode of antimicrobial action by Ag-NPs may be through the inhibition of microbial processes on the cell surface and within the cell. Previous research demonstrated that the Ag-NPs attach themselves to the cell membrane of an organism. This makes the membrane more permeable, leads to the dissipation of the cellular adenosine triphosphate pool through the proton motive force, and ultimately leads to cell death.[71,81]

The MIC values obtained on treatment with 5 mg/mL Ag-NP were 0.57, 0.42, 0.60, 0.61, 0.47, 0.43, 0.52, and 0.36 OD, respectively, against *S. typhi*, *P. vulgaris*, *S. sonnei*, *V. cholerae*, *P. aeruginosa*, *K. pneumoniae*, *E. aerogenes*, and *B. megaterium*. Treatment with 10 mg/mL Ag-NPs gave significant MIC values for all bacterial strains: *S. typhi* (0.47 OD), *B. subtilis* (0.34 OD), *P. vulgaris* (0.36 OD), *S. sonnei* (0.52 OD), *V. cholerae* (0.39 OD), *P. aeruginosa* (0.29 OD), *K. pneumoniae* (0.50 OD), *E. coli* (0.37 OD), *E. aerogenes* (0.51 OD), *B. cereus* (0.37 OD), and *B. megaterium*

Table 4 Antibacterial efficacy of biosynthesized Ag-NPs against different bacterial strains using time course growth assay and MIC

Samples and bacterial strains	Time course growth assay (OD 550 nm) Inhibition of bacterial growth at time intervals					MIC (OD 420 nm) 24 hours
	0 hour	1 hour	2 hours	3 hours	5 hours	
Ag-NPs (5 mg/mL)						
Salmonella typhi	0.23±0.01	0.28±0.01	0.29±0.01	0.30±0.01	0.48±0.04	0.57±0.02
Proteus vulgaris	0.15±0.01	0.16±0.00	0.16±0.00	0.17±0.00	0.26±0.04	0.42±0.02
Shigella sonnei	0.20±0.00	0.23±0.00	0.23±0.00	0.25±0.01	0.37±0.08	0.60±0.04
Vibrio cholerae	0.24±0.01	0.28±0.01	0.29±0.01	0.30±0.01	0.38±0.05	0.61±0.01
Pseudomonas aeruginosa	0.20±0.00	0.23±0.00	0.24±0.00	0.25±0.01	0.30±0.04	0.47±0.00
Klebsiella pneumoniae	0.17±0.03	0.20±0.05	0.20±0.05	0.22±0.06	0.40±0.08	0.43±0.16
Escherichia coli	0.18±0.00	0.20±0.00	0.20±0.00	0.20±0.00	0.35±0.02	1.40±0.10
Enterobacter aerogenes	0.15±0.01	0.17±0.00	0.18±0.00	0.18±0.00	0.29±0.04	0.52±0.06
Bacillus megaterium	0.15±0.01	0.16±0.01	0.16±0.01	0.17±0.01	0.31±0.01	0.36±0.00
Ag-NPs (10 mg/mL)						
S. typhi	0.19±0.00	0.24±0.01	0.25±0.01	0.26±0.01	0.41±0.01	0.47±0.01
Bacillus subtilis	0.17±0.01	0.19±0.01	0.19±0.01	0.20±0.01	0.40±0.01	0.34±0.01
P. vulgaris	0.16±0.01	0.17±0.01	0.17±0.01	0.18±0.01	0.27±0.06	0.36±0.02
S. sonnei	0.18±0.01	0.20±0.01	0.21±0.02	0.21±0.02	0.35±0.06	0.52±0.06
V. cholerae	0.15±0.01	0.18±0.01	0.18±0.01	0.19±0.01	0.38±0.04	0.39±0.01
P. aeruginosa	0.15±0.00	0.16±0.00	0.16±0.00	0.17±0.00	0.35±0.01	0.29±0.01
K. pneumoniae	0.15±0.00	0.17±0.01	0.18±0.00	0.18±0.01	0.29±0.06	0.50±0.04
E. coli	0.17±0.00	0.18±0.00	0.19±0.00	0.19±0.00	0.36±0.01	0.37±0.00
E. aerogenes	0.16±0.01	0.18±0.01	0.19±0.00	0.19±0.00	0.28±0.04	0.51±0.06
Bacillus cereus	0.13±0.00	0.16±0.00	0.17±0.00	0.17±0.01	0.37±0.02	0.37±0.01
B. megaterium	0.13±0.00	0.14±0.00	0.15±0.00	0.15±0.00	0.26±0.04	0.34±0.00
$AgNO_3$ (5 mg/mL)						
S. typhi	0.19±0.00	0.21±0.00	0.24±0.00	0.31±0.00	0.40±0.01	1.46±0.03
P. vulgaris	0.18±0.00	0.18±0.00	0.19±0.00	0.22±0.01	0.25±0.01	1.61±0.05
V. cholerae	0.18±0.00	0.17±0.00	0.18±0.00	0.19±0.00	0.19±0.00	1.59±0.09
P. aeruginosa	0.18±0.00	0.19±0.00	0.23±0.00	0.28±0.00	0.34±0.00	0.98±0.00
K. pneumoniae	0.17±0.00	0.17±0.00	0.18±0.00	0.20±0.00	0.23±0.00	0.92±0.15
Serratia marcescens	0.27±0.04	0.22±0.01	0.23±0.01	0.26±0.02	0.33±0.03	1.84±0.11
E. coli	0.25±0.02	0.25±0.02	0.27±0.02	0.31±0.03	0.31±0.04	1.88±0.37
E. aerogenes	0.42±0.01	0.20±0.01	0.19±0.01	0.19±0.01	0.20±0.01	0.19±0.01
B. cereus	0.42±0.03	0.19±0.00	0.19±0.00	0.21±0.01	0.21±0.00	0.24±0.03
B. megaterium	0.42±0.01	0.15±0.00	0.15±0.00	0.16±0.00	0.19±0.01	0.18±0.00
$AgNO_3$ (10 mg/mL)						
S. typhi	0.31±0.01	0.36±0.00	0.36±0.00	0.40±0.00	0.48±0.00	0.73±0.04
P. vulgaris	0.26±0.00	0.29±0.00	0.30±0.00	0.35±0.00	0.44±0.01	0.60±0.02
S. sonnei	0.19±0.01	0.20±0.01	0.24±0.00	0.27±0.00	0.30±0.00	0.68±0.06
V. cholerae	0.22±0.00	0.21±0.00	0.21±0.00	0.21±0.00	0.22±0.01	1.21±0.01
P. aeruginosa	0.22±0.01	0.21±0.01	0.21±0.01	0.21±0.00	0.22±0.00	0.92±0.02
K. pneumoniae	0.23±0.01	0.24±0.01	0.30±0.01	0.33±0.02	0.35±0.02	0.72±0.04
S. marcescens	0.18±0.00	0.19±0.00	0.17±0.00	0.21±0.00	0.25±0.00	0.99±0.06
E. coli	0.38±0.05	0.44±0.05	0.51±0.04	0.50±0.04	0.56±0.01	1.67±0.26
E. aerogenes	0.36±0.02	0.39±0.01	0.42±0.01	0.46±0.00	0.51±0.00	1.84±0.01
B. cereus	0.15±0.01	0.16±0.01	0.16±0.01	0.17±0.01	0.17±0.01	0.43±0.03
B. megaterium	0.38±0.00	0.37±0.01	0.36±0.01	0.38±0.01	0.45±0.02	1.63±0.01
Chloramphenicol (10 mg/mL)						
S. typhi	0.16±0.00	0.12±0.00	0.49±0.01	0.11±0.00	0.11±0.00	0.34±0.03
B. subtilis	0.16±0.01	0.14±0.00	0.38±0.01	0.13±0.00	0.13±0.00	0.25±0.03
P. vulgaris	0.14±0.00	0.14±0.00	0.13±0.00	0.34±0.00	0.45±0.01	0.89±0.01
S. sonnei	0.18±0.00	0.15±0.02	0.44±0.00	0.15±0.02	0.15±0.02	0.30±0.01
V. cholerae	0.16±0.00	0.12±0.00	0.34±0.07	0.12±0.00	0.12±0.00	0.29±0.01

(*Continued*)

Table 4 (*Continued*)

Samples and bacterial strains	Time course growth assay (OD 550 nm) Inhibition of bacterial growth at time intervals					MIC (OD 420 nm) 24 hours
	0 hour	1 hour	2 hours	3 hours	5 hours	
P. aeruginosa	0.16±0.01	0.12±0.00	0.37±0.01	0.13±0.00	0.12±0.00	0.26±0.01
K. pneumoniae	0.17±0.00	0.13±0.00	0.49±0.01	0.13±0.00	0.13±0.00	0.37±0.01
S. marcescens	0.16±0.00	0.12±0.00	0.55±0.02	0.13±0.00	0.13±0.00	0.46±0.03
E. coli	0.18±0.00	0.12±0.00	0.41±0.01	0.12±0.00	0.12±0.00	0.35±0.01
E. aerogenes	0.16±0.01	0.12±0.00	0.42±0.02	0.12±0.00	0.12±0.00	0.37±0.00
B. cereus	0.15±0.00	0.12±0.00	0.45±0.00	0.12±0.00	0.12±0.00	0.32±0.02
B. megaterium	0.17±0.00	0.13±0.00	0.49±0.01	0.14±0.00	0.14±0.00	0.44±0.03

Notes: All values are represented as mean ± SE of triplicate values and analyzed using SPSS 17.0 software with one-way ANOVA followed by DMRT and their relationship was considered to be statistically significant when $P<0.05$.

Abbreviations: $AgNO_3$, silver nitrate; Ag-NPs, silver nanoparticles; DMRT, Duncan's new multiple range test; MIC, minimum inhibitory concentration; SE, standard error; SPSS, Statistical Package for the Social Sciences; OD, optical density.

(0.34 OD). In an earlier study, Ag-NP treatment showed significant antibacterial activity, with MIC values of 6.25, 11.79, and 13.02 μg/mL, against *E. coli*, respectively.[82]

Gram-negative bacterial strains have a thin peptidoglycan layer (2–3 nm) between the cytoplasmic membrane and the outer membrane, while gram-positive bacteria lack an outer membrane and possess a peptidoglycan layer of about 30 nm thickness.[83] Hence, the gram-negative bacteria, *E. coli*, may have higher redox activity which may result in Ag-species forming cell particle aggregates.[71,84] Such an inhibitory effect of Ag-NPs against *E. coli* has been previously reported.[85] Thirumurugan et al[86] studied the antibacterial effects of Ag-NPs against *E. coli*, *S. typhi*, *K. pneumoniae*, *P. vulgaris*, and *B. subtilis* using standard disk diffusion and MIC methods. Moreover, Ag-NPs inhibit microbial growth by anchoring or penetrating bacterial cell walls and modulating cellular signaling by dephosphorylating the peptide substrates on tyrosine residues.[87] Ag-NPs have also been thought to be involved in DNA, RNA, and protein synthesis.[70,88] Earlier studies showed that Ag-NPs possess antimicrobial properties against *E. coli*,[35] *K. pneumoniae*,[89] *Enterobacter* sp.,[90] *S. aureus*,[35,91] and *B. subtilis*.[92] The positive control showed a great variation ranging from 0.25 to 0.89 OD; in this trial, chloramphenicol inhibited *B. subtilis*, *S. sonnei*, *V. cholerae*, and *P. aeruginosa*, with MIC values below 0.30 OD. Based on these results, we conclude that biosynthesized Ag-NPs might be used to formulate drugs to combat microbial diseases and spoilage.

In vivo anti-inflammatory activity

The development of edema in the rat paws after carrageenan injection is due to the release of histamine, serotonin, and prostaglandins, causing increased blood flow to the acutely inflamed areas, resulting in redness of the paw.[93,94] Numerous flavonoid components in medicinal ferns, including apigenin, luteolin, naringenin, and kaempferol, have been reported to exhibit strong antioxidant capacity. This activity results in clinical reactions such as reduced blood lipid levels, liver protection, resistance to inflammation, relaxed coronary arteries, and antibacterial activity.[95,96] Table 5 shows a summary of the anti-inflammatory potential of biosynthesized Ag-NPs at doses of 50 and 100 mg/kg body weight using oral route administration. Both doses exhibited significant anti-inflammatory activities by inhibiting edema by 47.59% and 56.36%, respectively (Figure 7), while the ethanol extract (200 and 400 mg/kg) of *P. tripartita* showed inhibition

Table 5 In vivo anti-inflammatory activity of biosynthesized Ag-NPs

Animal groups	Drugs (mg/kg)	0 hour	1 hour	2 hours	3 hours	24 hours
I	Normal (positive)	2.38±0.08	2.72±0.09	2.53±0.14	2.58±0.07	2.49±0.04
II	Carrageenan 10 (negative)	4.33±0.38	4.75±0.46	4.94±0.44	5.24±0.31	4.79±0.38
III	Indomethacin 10	2.55±0.13 (41.10%)	2.30±0.09 (51.57%)	2.53±0.13 (48.78%)	2.08±0.03 (60.30%)	1.48±0.11 (69.10%)
IV	Ag-NPs 50	3.19±0.03 (26.32%)	2.91±0.19 (38.73%)	2.85±0.28 (42.30%)	2.67±0.18 (49.04%)	2.51±0.16 (47.59%)
V	Ag-NPs 100	2.76±0.12 (36.25%)	2.70±0.17 (43.15%)	2.68±0.09 (45.74%)	2.57±0.10 (50.95%)	2.09±0.12 (56.36%)

Notes: All values are expressed as mean ± SE of six rats and analyzed using SPSS 17.0 software with one-way ANOVA followed by DMRT and their relationship was considered to be statistically significant when $P<0.05$.

Abbreviations: Ag-NPs, silver nanoparticles; ANOVA, analysis of variance; DMRT, Duncan's new multiple range test; SE, standard error; SPSS, Statistical Package for the Social Sciences.

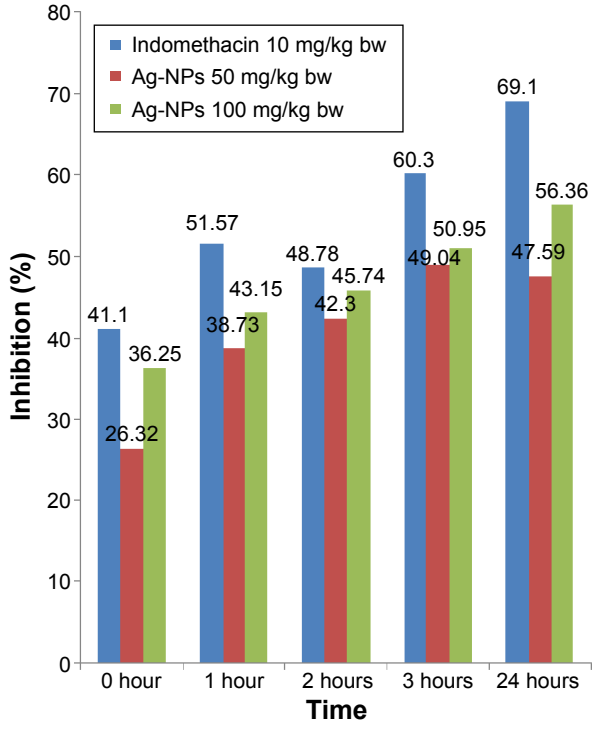

Figure 7 Percentage of inhibition of paw edema volume for anti-inflammatory activity.
Abbreviations: Ag-NPs, silver nanoparticles; bw, body weight.

of 62.63% and 48.64%, respectively (unpublished data). The anti-inflammatory activity in biosynthesized Ag-NPs is dose dependent, while the activity of the *P. tripartita* extract is dose independent. In previous studies, the maximum percentage of edema inhibition was exhibited by Ag-NPs at 50 mg/kg body weight.[58,97] Other ferns, including *Equisetum arvense*, *Cyathea phalerata*, and *Blechnum occidentale*, have also been shown to display anti-inflammatory and antioxidant activity due to the presence of secondary metabolites like phenolic compounds.[98,99] Over the duration of this study, no deaths occurred in any of the experimental groups. Moreover, the extracts did not induce morphological variations or any toxic signs in the animal subjects.

Conclusion

In this study, we report a protocol for a cost-effective and ecofriendly method of reducing silver ions using *P. tripartita* leaf extract. We also performed characterization of the resulting Ag-NPs. Morphologically, the biosynthesized Ag-NPs were <100 nm in size. Our data show that the aqueous leaf extract of *P. tripartita* Sw. is suitable for the rapid synthesis of Ag-NPs, since it possesses diverse groups of phytochemicals including phenols, flavonoids, tannins, terpenoids, reducing sugars, and proteins. Due to significant antioxidant, anti-inflammatory, and antimicrobial properties of Ag-NPs biosynthesized from *P. tripartita*, this extract may be effectively used as a natural plant-based drug. However, further pharmacological studies should be carried out to validate our in vitro results. Further studies are also needed to determine and characterize the chemical constituents of the extract, as well as to find the mechanism of action responsible for these properties.

Disclosure

The authors report no conflicts of interest in this work.

References

1. Ratnam DV, Ankola DD, Bhardwaj V, Sahana DK, Kumar MN. Role of antioxidants in prophylaxis and therapy: a pharmaceutical perspective. *J Control Release*. 2006;113:189–207.
2. Amendola V, Polizzi S, Meneghetti M. Free Silver nanoparticles synthesized by laser ablation in organic solvents and their easy functionalization. *Langmuir*. 2007;23:6766–6770.
3. Fernandez EJ, Garcia-Barrasa J, Laguna A, Lopez-de-Luzuriaga J, Monge M, Torres C. The preparation of highly active antimicrobial silver nanoparticles by an organometallic approach. *Nanotechnology*. 2008; 19(18):1–6.
4. Vedpriya A. Living Systems: eco-friendly nanofactories. *Dig J Nanomater Biostruct*. 2010;5(1):9–21.
5. Satyavani K, Ramanathan T, Gurudeeban S. Green synthesis of silver nanoparticles by using stem derived callus extract of bitter apple (Citrullus colocynthis). *Dig J Nanomater Biostruct*. 2011;6(3):1019–1024.
6. Murphy CJ. Sustainability as a design criterion in nanoparticle synthesis and applications. *J Mater Chem*. 2008;18:2173–2176.
7. Silver S, Phung LT, Silver G. Silver as biocides in burn and wound dressings and bacterial resistance to silver compounds. *J Ind Microbiol Biotechnol*. 2006;33(7):627–634.
8. Konishi Y, Ohno K, Saitoh N, et al. Bioreductive deposition of platinum nanoparticles on the bacterium Shewanella algae. *J Biotechnol*. 2007;128(3):648–653.
9. Willner I, Baron R, Willner B. Growing metal nanoparticles by enzymes. *Adv Mater*. 2006;18(9):1109–1120.
10. Vigneshwaran N, Ashtaputre NM, Varadarajan PV, Nachane RP, Paraliker KM, Balasubramanya RH. Biological synthesis of silver nanoparticles using the fungus Aspergillus flavus. *Mater Lett*. 2007;61: 1413–1418.
11. Shankar SS, Rai A, Ahmad A, Sastry M. Rapid synthesis of Au, Ag, and bimetallic Au core–Ag shell nanoparticles using neem (Azadirachta indica) leaf broth. *J Colloid Interface Sci*. 2004;275(2):496–502.
12. Jae Y, Beom SK. Rapid biological synthesis of silver nanoparticles using plant leaf extracts. *Bioprocess Biosyst Eng*. 2009;32(1):79–84.
13. Jha AK, Prasad K. Green synthesis of silver nanoparticles using Cycas leaf. *Int J Green Nanotechnol Phys Chem*. 2010;1(2):110–117.
14. Vivek M, Senthil Kumar P, Steffi S, Sudha S. Biogenic silver nanoparticles by *Gelidiella acerosa* extract and their antifungal effects. *Avicenna J Med Biotech*. 2011;3(3):143–148.
15. Gardea-Torresdey JL, Gomez E, Peralta-Videa JR, Parsons JG, Troiani H, Jose-Yacaman M. Alfalfa sprouts: a natural source for the synthesis of silver nanoparticles. *Langmuir*. 2003;19:1357–1361.
16. Kumar V, Yadav SK. Plant mediated synthesis of silver and gold nanoparticles and their applications. *J Chem Technol Biotechnol*. 2009; 84(2):151–157.
17. Baskaran X, Jeyachandran R, Melghias G. In vitro spore germination and gametophytic growth development of a critically endangered fern Pteris tripartita Sw. *Afr J Biotechnol*. 2014;13(23):2350–2358.
18. Baskaran X, Jeyachandran R. In vitro spore germination and gametophyte growth assessment of a critically endangered fern: Pteris tripartita Sw. *Pteridol Res*. 2012;1(1):4–9.

19. Baskaran X, Geo Vigila A, Rajan K, Jeyachandran R. Apogamous sporophyte development through spore reproduction of a South Asia's critically endangered fern: Pteris tripartita Sw. *Asian Pac J Reprod*. 2015;4(2):135–139.
20. Baskaran X, Jeyachandran R. Evaluation of antioxidant and phytochemical analysis of Pteris tripartita Sw. a critically endangered fern from South India. *J Fairylake Bot Gard*. 2010;9(3):28–34.
21. Baskaran X. *DNA Sequencing, Micropropagation and Pharmacological Evaluation of Pteris Tripartita Sw. – a Critically Endangered Fern* [PhD dissertation]. Tiruchirapalli, India: Bharathidasan University; 2013.
22. Song JY, Kim BS. Rapid biological synthesis of silver nanoparticles using plant leaf extracts. *Bioprocess Biosyst Engg*. 2009;32(1):79–84.
23. Hemali P, Pooja M, Sumitra C. Green synthesis of silver nanoparticles from marigold flower and its synergistic antimicrobial potential. *Arab J Chem*. 2015;8(5):732–741.
24. Blois MS. Antioxidants determination by the use of a stable free radical. *Nature*. 1958;26:1199–1200.
25. Dinis TCP, Madeira VMC, Almeida LM. Action of phenolic derivatives (acetoaminophen, salycilate, and 5-aminosalycilate) as inhibitors of membrane lipid peroxidation and as peroxyl radical scavengers. *Arch Biochem Biophys*. 1994;315(1):161–169.
26. Prieto P, Pineda M, Aguilar M. Spectrophotometric quantitative of antioxidant capacity through the formation of a phosphomolybdenum complex: Specific application to the determination of vitamin E. *Anal Biochem*. 1999;269(2):337–341.
27. Re R, Pellegrini N, Proteggente A, Pannala A, Yang M, Rice-Evans C. Antioxidant activity applying an improved ABTS radical cation decolorization assay. *Free Radic Biol Med*. 1999;26(9–10):1231–1237.
28. Ruch RJ, Cheng SJ, Klaunig JE. Prevention of cytotoxicity and inhibition of intercellular communication by antioxidant catechins isolated from Chinese green tea. *Carcinogenesis*. 1989;10(6):1003–1008.
29. Rabe T, Staden V. Isolation of an antibacterial sesquiterpenoid from Warbugia salutaris. *J Ethnopharmacol*. 2000;73(1–2):171–174.
30. Taylor RSL, Manandhar NP, Towers GHN. Screening of selected medicinal plants of Nepal for antimicrobial activities. *J Ethnopharmacol* 1995;46(3):153–159.
31. Palombo EA, Semple SJ. Antibacterial activity of traditional Australian medicinal plants. *J Ethnopharmacol*. 2001;77(2–3):151–157.
32. Barry AL, Thornsberry C. Susceptibility test: diffusion test procedures. In: Balows A, Hazsler WJ, Herrmann KL, Isenberg HD, Shadomy HJ, editors. *Manual of Clinical Microbiology*. 5th ed. Washington: American Society of Microbiology; 1991:463–474.
33. Ecobicon DJ. *The Basis of Toxicology Testing*. New York: CRC Press; 1997.
34. Winter CA, Risley EA, Nuss GW. Carrageenan-induced edema in hind paw of rats as an assay for anti-inflammatory drugs. *Proc Soc Exp Biol Med*. 1962;111:544–547.
35. Prasad TNVKV, Elumalai EK, Khateeja S. Evaluation of the antimicrobial efficacy of phytogenic silver nanoparticles. *Asian Pac J Trop Biomed*. 2011:S82–S85.
36. Sarkar R, Kumbhakar P, Mitra AK. Green synthesis of silver nanoparticles and its optical properties. *Dig J Nanomater Biostruct*. 2010;5:491–496.
37. Fathima SR, Vadivel A, Samuthira N, Mirunalini S. Antiproliferative effect of silver nanoparticles synthesized using amla on Hep2 cell line. *Asian Pac J Trop Med*. 2013;6(1):1–10.
38. Prasad TNVKV, Elumalai EK. Biofabrication of Ag nanoparticles using *Moringa oleifera* leaf extract and their antimicrobial activity. *Asian Pac J Trop Biomed*. 2011;1(6):439–442.
39. Vigneshwaran N, Kathe A, Varadrajan PV, Nachane RP, Balasubramanya RH. Biomimetics of silver nanoparticles by white rot fungi Phaenerochaete chrysosporium. *Colloids Surf B Biointerfaces*. 2006;53(1):55–59.
40. Panneerselvam C, Ponarulselvam S, Murugan K, Kalimuthu K, Thangamani S. Synthesis of silver nanoparticles using leaves of Catharanthus roseus Linn. G.Donn and their antiplasmodial activities. *Asian Pac J Trop Biomed*. 2012;2(7):574–580.
41. Lakshmi YSG, Banu F, Ezhilarasan M, Arumugam D, Sahadevan D. *Green Synthesis of Silver Nanoparticles from Cleome viscosa: Synthesis and Antimicrobial Activity*. Singapore: International Conference on Bioscience, Biochemistry and Bioinformatics (IACSIT Press). 2011;334–337.
42. Suriya J, Bharathi Raja S, Sekar V, Rajasekaran R. Biosynthesis of silver nanoparticles and its antibacterial activity using seaweed Urospora sp. *Afr J Biotechnol*. 2012;11(58):12192–12198.
43. Stuart B. *Infrared Spectroscopy: Fundamentals and Applications*. Weinheim: Wiley-VCH Verlag Gmbh & Co. KGaA; 2004.
44. Tian N, Liu Z, Huang J, Luo G, Liu S, Liu X. Isolation and preparation of flavonoids from the leaves of Nelumbo nucifera Gaertn. by preparative reversed-phase high-performance liquid chromatography. *Se Pu*. 2007;25(1):88–92.
45. Li S, Shen Y, Xie A. Green synthesis of silver nanoparticles using Capsicum annuum L. extract. *Green Chem*. 2007;9:852–858.
46. Ogi T, Saitoh N, Nomura T, Konishi Y. Room-temperature synthesis of gold nanoparticles and nanoplates using Shewanella algae cell extract. *J Nanopart Res*. 2010;12(7):2531–2539.
47. Chung IM, Park I, Seung-Hyun K, Thiruvengadam M, Rajakumar G. Plant-mediated synthesis of silver nanoparticles: their characteristic properties and therapeutic applications. *Nanoscale Res Lett*. 2016;11:40.
48. Qureshi MZ, Bashir T, Khursheed S, et al. Green synthesis of nanosilver particles from extract of Eucalyptus citriodora and their characterization. *Asian J Chem*. 2014;26(7):1–3.
49. Amutha M, Lalitha P, Firdhouse MJ. Biosynthesis of silver nanoparticles using Kedrostis foetidissima (Jacq.) Cogn. *J Nanotechnol*. 2014;2014:5.
50. Marslin G, Selvakesavan RK, Franklin G, Sarmento B, Dias ACP. Antimicrobial activity of cream incorporated with silver nanoparticles biosynthesized from *Withania somnifera*. *Int J Nanomed*. 2015;10:5955–5963.
51. Gurunathan S, Jeong JK, Han JW, Zhang XF, Park JH, Kim JH. Multidimensional effects of biologically synthesized silver nanoparticles in Helicobacter pylori, Helicobacter felis, and human lung (L132) and lung carcinoma A549 cells. *Nanoscale Res Lett*. 2015;10:35.
52. Singh K, Panghal K, Kadyan S, Chaudhary U, Yadav JP. Green silver nanoparticles of Phyllanthus amarus: as an antibacterial agent against multi drug resistant clinical isolates of Pseudomonas aeruginosa. *J Nanobiotech*. 2014;12:40.
53. Nabikhan A, Kandasamy K, Raj A, Alikunhi NM. Synthesis of antimicrobial silver nanoparticles by callus and leaf extracts from salt marsh plant, Sesuvium portulacastrum L. *Colloids Surf B Biointerfaces*. 2010;79(2):488–493.
54. Geethalakshmi R, Sarada DVL. Synthesis of plant-mediated silver nanoparticles using Trianthema decandra extract and evaluation of their anti-microbial activities. *Int J Eng Sci Tech*. 2010;2(5):970–975.
55. Dehpour AA, Ebrahimzadeh MA, Nabavi SF, Nabavi SM. Antioxidant activity of methanol extract of Ferula asafoetida and its essential oil composition. *Grasas y Aceites*. 2009;60(4):405–412.
56. Bhakya S, Muthukrishnan S, Sukumaran M, Muthukumar M. Biogenic synthesis of silver nanoparticles and their antioxidant and antibacterial activity. *Appl Nanosci*. 2015;6(5):755–766
57. Chandra Mohan S, Sasikala K, Anand T, Vengaiah PC, Krishnaraj S. Green synthesis, antimicrobial and antioxidant effects of silver nanoparticles using Canthium coromandelicum leaves extract. *Res J Microbiol*. 2014;9(3):142–150.
58. El-Rafie HM, Hamed MAA. Antioxidant and anti-inflammatory activities of silver nanoparticles biosynthesized from aqueous leaves extracts of four Terminalia species. *Adv Nat Sci Nanosci Nanotechnol*. 2014;5(3):35008.
59. Niraimathi KL, Sudha V, Lavanya R, Brindha P. Biosynthesis of silver nanoparticles using Alternanthera sessilis (Linn.) extract and their antimicrobial, antioxidant activities. *Colloids Surf B Biointerfaces*. 2013;102(1):288–291.
60. Vishnu KM, Murugesan S. In vitro antioxidant activity of silver nanoparticles from Colpomenia sinuosa and Halymenia poryphyroides. *World J Pharm Sci*. 2014;2(8):817–820.

61. Inbathamizh L, Mekalai Ponnu T, Jancy Mary E. In vitro evaluation of antioxidant and anticancer potential of Morinda pubescens synthesized silver nanoparticles. *J Pharm Res*. 2013;6:32–38.
62. Preeti D, Mausumi M. In-vitro free radical scavenging activity of biosynthesized gold and silver nanoparticles using Prunus armeniaca (apricot) fruit extract. *J Nanoparticle Res*. 2013;15:1366.
63. Kalaiyarasu T, Karthi N, Sharmila Gowri V, Manju V. In vitro assessment of antioxidant and antibacterial activity of green synthesized silver nanoparticles from Digitaria radicosa leaves. *Asian J Pharm Clin Res*. 2016:9(1):297–302.
64. Wang TC, Lee HI, Yang CC. Evaluation of in vitro antioxidant and anti-lipid peroxidation activities of Ching-Pien-Tsao (Pteris multifida Poiret). *J Taiwan Agric Res*. 2009;58(1):55–60.
65. Gulcin I, Elmastas M, Aboul-Enein HY. Determination of antioxidant and radical scavenging activity of basil (Ocimum basilicum L. family Lamiaceae) assayed by different methodologies. *Phytother Res*. 2007; 21(4):354–361.
66. Lee SK, Mbwambo ZH, Chung H. Evaluation of the antioxidant potential of natural products. *Comb Chem High Throughput Screen*. 1998;1(1):35–46.
67. Fabrega J, Fawcett SR, Renshaw JC, Lead JR. Silver nanoparticle impact on bacterial growth: effect of pH, concentration and organic matter. *Environ Sci Tech*. 2009;43(19):7285–7290.
68. Fabrega J, Renshaw JC, Lead JR. Interactions of silver nanoparticles with Pseudomonas putida biofilms. *Environ Sci Technol*. 2009; 43(23):9004–9009.
69. Shahverdi AR, Fakhimi A, Shahverdi HR, Minaian S. Synthesis and effect of Silver nanoparticles on the antibacterial activity of different antibiotics against Staphylococcus aureus and Escherichia coli. *Nanomed Nanotechnol*. 2007;3(2):168–171.
70. Panacek A, Kvitek L, Prucek R, et al. Silver colloid nanoparticles: synthesis, characterization and their antibacterial activity. *J Phys Chem B*. 2006;110(33):16248–16253.
71. Sondi I, Salopek-Sondi B. Silver nanoparticles as antimicrobial agent: a case study on E. coli as a model for Gram-negative bacteria. *J Colloid Interface Sci*. 2004;275(1):177–182.
72. Panacek A, Kolar M, Vecerova R. et al. Antifungal activity of Silver nanoparticles against Candida spp. *Biomaterials*. 2009;30(31): 6333–6340.
73. Bruins RM, Kapil S, Oehme SW. Microbial resistance to metals in the environment. *Ecotoxicol Environ Safe*. 2000;45(3):198–207.
74. Roy S, Rao K, Bhuvaneswari C, Giri A, Mangamoori LN. Phytochemical analysis of Andrographis paniculata extract and its antimicrobial activity. *World J Microbiol Biotech*. 2010;26:85–91.
75. Dibrov P, Dzioba J, Gosink KK, Hase CC. Chemiosmotic mechanism of antimicrobial activity of Ag(+) in Vibrio cholerae. *Antimicrob Agents Chemother*. 2002;46(8):2668–2670.
76. Pal S, Tak YK, Song JM. Does the antibacterial activity of silver nanoparticles depend on the shape of the nanoparticle? A study of the gram-negative bacterium Escherichia coli. *Appl Environ Microbiol*. 2007; 73(6):1712–1720.
77. Arora S, Jain J, Rajwade JM, Paknikar KM. Cellular responses induced by silver nanoparticles: In vitro studies. *Toxicol Lett*. 2008;179(2): 93–100.
78. Hindi KM, Ditto AJ, Panzner MJ, et al. The antimicrobial efficacy of sustained release silver–carbene complex-loaded L-tyrosine polyphosphate nanoparticles: characterization, in vitro and in vivo studies. *Biomaterials*. 2009;30(22):3771–3779.
79. Anzano M, Tosti A, Lasagni M, Campiglio A, Pitea D, Collina E. Antimicrobial activity of thin metallic silver flakes, waste products of a manufacturing process. *J Environ Sci*. 2011;23(9):1570–1577.
80. Yoon KY, Byeon JH, Park JH, Hwang J. Susceptibility constants of Escherichia coli and Bacillus subtilis to silver and copper nanoparticles. *Sci Total Environ*. 2007;373(2–3):572–575.
81. Lok CN, Ho CM, Chen R, et al. Proteomic analysis of the mode of antibacterial action of silver nanoparticles. *J Proteome Res*. 2006;5(4): 916–924.
82. Castanon GAM, Martınez NN, Gutierrez FM, Mendoza JRM, Ruiz F. Synthesis and antibacterial activity of Silver nanoparticles with different sizes. *J Nanopart Res*. 2008;10(8):1343–1348.
83. Shockman GD, Barret JF. Structure, function, and assembly of cell walls of gram-positive bacteria. *Annu Rev Microbiol*. 1983;37:501–527.
84. Kahraman M, Yazici MM, Sahin F, Bayrak OF, Culha M. Reproducible surface-enhanced Raman scattering spectra of bacteria on aggregated silver nanoparticles. *Appl Spectrosc*. 2007;61(5):479–485.
85. Choi O, Deng KK, Kim NJ, Ross L, Surampallie RY, Hu Z. The inhibitory effects of silver nanoparticles, silver ions and silver chloride colloids on microbial growth. *Water Res*. 2008;42(12):3066–3074.
86. Thirumurugan G, Shaheedha SM, Dhanaraju MD. In-vitro evaluation of anti-bacterial activity of silver nanoparticles synthesised by using Phytophthora infestans. *Int J ChemTech Res*. 2009;1(3):714–716.
87. Shrivastava S, Bera T, Roy A, Singh G, Ramachandrarao P, Dash D. Characterization of enhanced antibacterial effects of novel silver nanoparticles. *Nanotechnology*. 2007;18(22):225103–225112.
88. Marini M, De Niederhausern N, Iseppi R, Bondi M, Sabia C, Toselli M. Antibacterial activity of plastics coated with silver dapped organic hybrid coatings prepared by sol-gel process. *Biomacromolecules*. 2007; 8(4):1246–1254.
89. Narges M, Shahram D, Seyedali S, et al. Biological synthesis of very small Silver nanoparticles by culture supernatant of Klebsiella pneumoniae: the effects of visible-light irradiation and the liquid mixing process. *Mater Res Bull*. 2009;44:1415–1421.
90. Ahmad RS, Sara M, Hamid RS, Hossein J, Ashraf-Asadat N. Rapid synthesis of Silver nanoparticles using culture supernatants of Enterobacteria: a novel biological approach. *Process Biochem*. 2007;42(5):919–923.
91. Nanda A, Saravanan M. Biosynthesis of silver nanoparticles from Staphylococcus aureus and its antimicrobial activity against MRSA and MRSE. *Nanomedicine*. 2009;5(4):452–456.
92. Saifuddin N, Wong CW, Yasumira AAN. Rapid biosynthesis of silver nanoparticles using culture supernatant of bacteria with microwave irradiation. *E J Chem*. 2009;6(1):61–70.
93. Georgewill OA, Georgewill UO. Evaluation of the anti-inflammatory activity of extract of Vernonia amygdalina. *Asia Pac J Trop Med*. 2010;3(2):150–151.
94. Foyet HS, Abdou BA, Ponka R, Asongalem AE, Kamtchouing P, Nastasa V. Effects of Hibiscus asper leaves extracts on carrageenan induced oedema and complete Freund's adjuvant induced arthritis in rats. *J Cell Anim Biol*. 2011;5(5):69–75.
95. Milovanovic V, Radulovic N, Todorovic Z, Stankovic M, Stojanovic G. Antioxidant, antimicrobial and genotoxicity screening of hydro-alcoholic extracts of five Serbian equisetum species. *Plant Food Hum Nutr*. 2007;62(3):113–119.
96. Ho R, Teai T, Bianchini JP, Lafont R, Raharivelomanana P. Ferns: from traditional uses to pharmaceutical development, chemical identification of active principles. In: Ashwani K, Helena F, Maria AR, editors. *Working with Ferns: Issues and Applications*. New York: Springer Science+Business Media, LLC; 2010:321–346.
97. David L, Moldovan B, Vulcu A, et al. Green synthesis, characterization and anti-inflammatory activity of silver nanoparticles using European black elderberry fruits extract. *Colloids Surf B Biointerfaces*. 2014;122:767–777.
98. Do Monte FHM, Santos JJG, Russi M, Lanziotti VMNB, Leal LKAM, Cunha GMA. Antinociceptive and anti-inflammatory properties of the hydroalcoholic extract of stems from Equisetum arvense L. in mice. *Pharmacol Res*. 2004;49(3):239–243.
99. Nonato FR, Barros TAA, Luchesse AM. Anti-inflammatory and antinociceptive activities of Blechnum occidentale L. extract. *J Ethnopharmacol*. 2009;125(1):102–107.